Fragile structural transition in Mo_3Sb_7

J.-Q. Yan,[1,2] M. A. McGuire,[1] A. F. May,[1] D. Parker,[1] D. G. Mandrus,[1,2] and B. C. Sales[1]
[1]*Materials Science and Technology Division, Oak Ridge National Laboratory, Oak Ridge, Tennessee 37831, USA*
[2]*Department of Materials Science and Engineering, University of Tennessee, Knoxville, Tennessee 37996, USA*
(Received 26 May 2015; revised manuscript received 20 July 2015; published 10 August 2015)

Mo_3Sb_7 single crystals lightly doped with Cr, Ru, or Te are studied in order to explore the interplay between superconductivity, magnetism, and the cubic-tetragonal structural transition. The structural transition at 53 K is extremely sensitive to Ru or Te substitution which introduces additional electrons, but robust against Cr substitution. No sign of a structural transition was observed in superconducting $Mo_{2.91}Ru_{0.09}Sb_7$ and $Mo_3Sb_{6.975}Te_{0.025}$. In contrast, 3 at.% Cr doping only slightly suppresses the structural transition to 48 K while leaving no trace of superconductivity above 1.8 K. Analysis of magnetic properties suggests that the interdimer interaction in Mo_3Sb_7 is near a critical value and essential for the structural transition. All dopants suppress the superconductivity of Mo_3Sb_7. The tetragonal structure is not necessary for superconductivity.

DOI: 10.1103/PhysRevB.92.064507 PACS number(s): 74.62.Dh, 61.50.Ks, 74.70.Ad, 81.10.Dn

I. INTRODUCTION

The interplay between structure, magnetism, and superconductivity has been an active topic in the condensed matter community for decades. For a variety of materials, superconductivity is found near a magnetic instability as a function of chemical doping or pressure. This has been well demonstrated in high-T_c cuprates and pniticides. Doping charge carriers, either holes or electrons, suppresses the antiferromagnetic order in cuprates or magnetic spin density wave transition in pniticides, and induces superconductivity. The suppression of magnetism and appearance of superconductivity are associated with a structural transition from a high temperature tetragonal phase to a low-temperature orthorhombic phase in both cuprates and pniticides. Thus, systems with magnetic and/or structural instabilities have been a fertile ground for looking for new superconductors. However, despite a tremendous effort in the last 30 years, the close interplay between magnetism, superconductivity, and structure and the mechanism mediating pairing are still under intense debate.

Despite a low $T_c \sim 2.08$ K [1], the Zintl compound Mo_3Sb_7 appears to show a close interplay between magnetism, structure, and superconductivity. Cooling across $T_t = 53$ K, the nearest neighbor (NN) Mo-Mo distance along the crystallographic c axis shortens leading to a structural transition from a high temperature Ir_3Ge_7-type cubic structure (space group $Im\bar{3}m$) to a low-temperature tetragonal ($I4/mmm$) structure [2,3]. This low-temperature tetragonal phase has been suggested to be beneficial for the low-temperature superconductivity [4]. It was suggested that the structural transition leads to the formation of spin singlet dimers, valence-bond crystal, and the opening of a spin gap of 120 K [2,3,5–7]. The effect of the spin gap on superconductivity might be rather weak, and possible spin fluctuations were argued to coexist with superconductivity [8,9]. A previous study on the transport and magnetic properties under hydrostatic pressure up to 22 kbar showed that T_t decreases while T_c increases with increasing pressure [10]. This resembles the pressure dependence of T_t and T_c of V_3Si with the A15 structure and AFe_2As_2 (A = Ca, Sr, and Ba) superconductors [11–13]. Moreover, a spin density wave state was suggested under high pressure that competes with superconductivity [10]. While high pressure studies on high quality single crystals are needed to confirm the appearance of this spin density wave state, there is ample evidence supporting the close correlation between magnetism, structure, and superconductivity in Mo_3Sb_7.

The effect of Te/Ru doping at high doping concentrations for $Mo_{3-x}Ru_xSb_7$ ($x = 0.25$, 0.50, and 1.0) and $Mo_3Sb_{7-x}Te_x$ ($x = 0.30$, 1.0, 1.60, and 2.2) has been studied both experimentally and theoretically [14–17]. Electronic structure calculations suggest a rigid-band behavior, where Te or Ru doping moves the Fermi level toward the valence band edge. This is supported by the observation that Mo_3Sb_7 changes from a paramagnetic metal to a diamagnetic semiconductor with increasing Te or Ru doping. Neither superconductivity, structural transition, nor spin gap was observed in heavily doped Mo_3Sb_7 [16,17]. To the best of our knowledge, no detailed study has been performed to explore the correlation between superconductivity, the structural transition, and magnetism in lightly doped compositions.

In this paper we report the effect of light doping on the structural transition, superconductivity, and magnetism of Mo_3Sb_7. Our results show that the structural transition of Mo_3Sb_7 is extremely sensitive to charge doping. No sign of a structural transition was observed in the normal state of $Mo_{2.91}Ru_{0.09}Sb_7$ (3% Ru doping) and $Mo_3Sb_{6.975}Te_{0.025}$ (0.36% Te doping), but the structural transition is rather robust against Cr doping. Data analysis discussed below suggests that the interdimer interaction in Mo_3Sb_7 is close to a critical value and essential for the occurrence of the structural transition. All dopants suppress superconductivity. Our superconducting and cubic Ru- and Te-doped crystals show that the low-temperature tetragonal phase is not a prerequisite for the occurrence of superconductivity.

II. EXPERIMENTAL DETAILS

All crystals were grown out of Sb flux as reported before [18]. The starting metal powder (Mo, Cr, and Ru) was reduced in flowing Ar balanced with 4% H_2 for 12 h at 1000 °C before using. To grow doped compositions, Mo or Sb was partially replaced by the desired dopant in the starting materials. The charge/flux ratio of 1:49 was used for

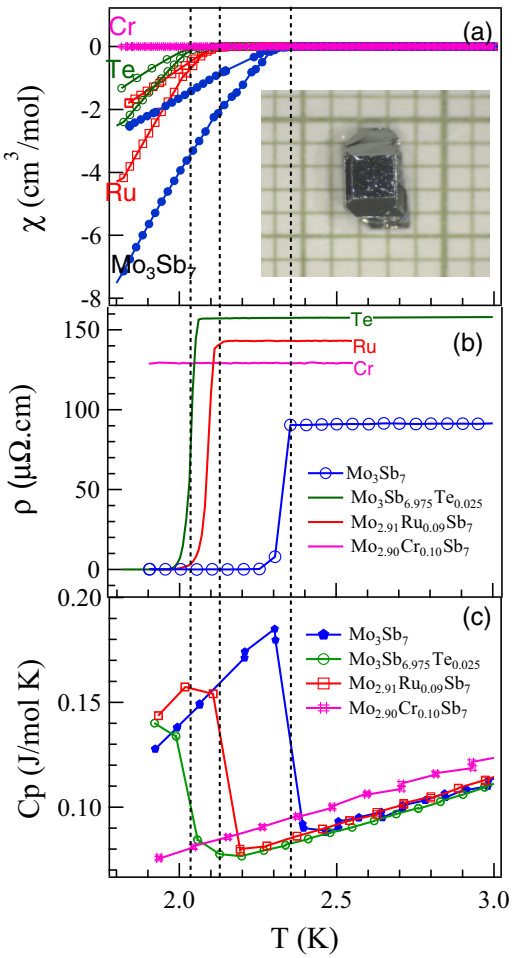

FIG. 1. (Color online) (a) Temperature dependence of magnetic susceptibility around T_c measured under an applied magnetic field of 10 Oe in both zero-field-cooling and field-cooling modes. Inset shows the photograph of a $Mo_{2.90}Cr_{0.10}Sb_7$ single crystal on a millimeter grid. (b) Temperature dependence of electrical resistivity around T_c. (c) Temperature dependence of specific heat around T_c. Data for Mo_3Sb_7 are replotted from Ref. [18]. Vertical dashed lines highlight the superconducting transition temperatures.

all compositions. For Ru- and Te-doped compositions, the crystals are well separated from residual flux after decanting at 700 °C. However, Cr-doped crystals are normally covered with a layer of Sb flux. This layer of residual flux can be removed mechanically with a surgical blade. Inset of Fig. 1(a) shows a Cr-doped Mo_3Sb_7 single crystal after cleaning the residual flux. For the growth of $Mo_{3-x}Cr_xSb_7$ with $x \geqslant 1$ in starting materials, the crystals are small with the largest dimension in submillimeter range and are normally covered with a thick layer of residual flux. These observations suggest that Cr dopant significantly increases the liquid's melting temperature.

Elemental analysis of the crystals was performed using a Hitachi TM-3000 tabletop electron microscope equipped with a Bruker Quantax 70 energy dispersive x-ray (EDX) system. X-ray diffraction on oriented single crystals and on powder from ground crystals was performed on a PANalytical X'Pert Pro MPD powder x-ray diffractometer using Cu $K_{\alpha 1}$ radiation. Magnetic properties were measured with a Quantum Design (QD) Magnetic Property Measurement System in the temperature range $1.8 \leqslant T \leqslant 300$ K. The temperature dependent specific heat and electrical transport data were collected using a 9 T QD Physical Property Measurement System.

The density-of-states and additional electrons relative to the stoichiometric compound were calculated from the converged WIEN2K band structure, as performed and presented in Ref. [19]. A very large number of k points—as many as 100 000 in the full Brillouin zone—were used to evaluate the density-of-states, and appropriate k-point convergence tests were performed. The number of additional electrons is determined by integrating the density-of-states, which amounts to the assumption of rigid band behavior in the addition of dopants such as Ru or Te. For the purposes of determining the experimental doping levels of Ru and Te, each Ru (substituting for Mo) is assumed to donate two additional electrons to the system, as was found by an explicit supercell calculation in Ref. [19], while Te (substituting for Sb) was assumed to donate one additional electron to the system, consistent with the observed approach to a semiconducting state induced by Te doping.

III. RESULTS AND DISCUSSIONS

Room temperature x-ray powder diffraction (not shown) confirmed the single phase for all compositions studied. In order to correlate the physical properties with the real dopant content x rather than the nominal one x_{nominal}, elemental analysis was performed with EDX. x was obtained by averaging the x values measured at five different locations on each sample. For Te-doped crystals studied in this work, our EDX does not have the resolution to resolve such a small amount of Te. Thus we use the nominal composition in the text. For a Ru-doped compound with the nominal composition $Mo_{2.91}Ru_{0.09}Sb_7$, x determined equals x_{nominal}. A significant difference between the real and nominal compositions was observed for a Cr-doped crystal where $Mo_{2.90}Cr_{0.10}Sb_7$ was obtained starting with the nominal $Mo_{2.70}Cr_{0.30}Sb_7$. Considering the observation that Cr-doped crystals cannot be well separated from flux by centrifuging at 700 °C, Cr might have a limited solubility in Sb flux at the growth temperatures. If all Cr starting materials are dissolved in Sb flux, the compositional difference suggests a distribution coefficient of Cr $k_{\text{eff}} = C_L/C_S > 1$, where k_{eff} is the distribution coefficient, and C_L and C_S are the concentrations of Cr in the melt and crystals.

Figure 1(a) shows the temperature dependence of magnetic susceptibility measured at a magnetic field of 10 Oe in both zero-field-cooling and field-cooling modes. T_c was suppressed from 2.35 K for Mo_3Sb_7 to 2.15 K for $Mo_{2.91}Ru_{0.09}Sb_7$ and 2.05 K for $Mo_3Sb_{6.975}Te_{0.025}$, respectively. No superconductivity was observed for $Mo_{2.90}Cr_{0.10}Sb_7$ above 1.80 K. The suppression of superconductivity with doping was further supported by the temperature dependence of the electrical resistivity [Fig. 1(b)] and specific heat [Fig. 1(c)].

Figure 2 shows the temperature dependence of magnetic susceptibility $\chi(T)$ measured under a field of 60 kOe. The magnetic susceptibility of Mo_3Sb_7, $Mo_3Sb_{6.975}Te_{0.025}$, and $Mo_{2.91}Ru_{0.09}Sb_7$ show similar temperature dependence. $Mo_{2.90}Cr_{0.10}Sb_7$ exhibits a strong Curie-Weiss (CW) tail below

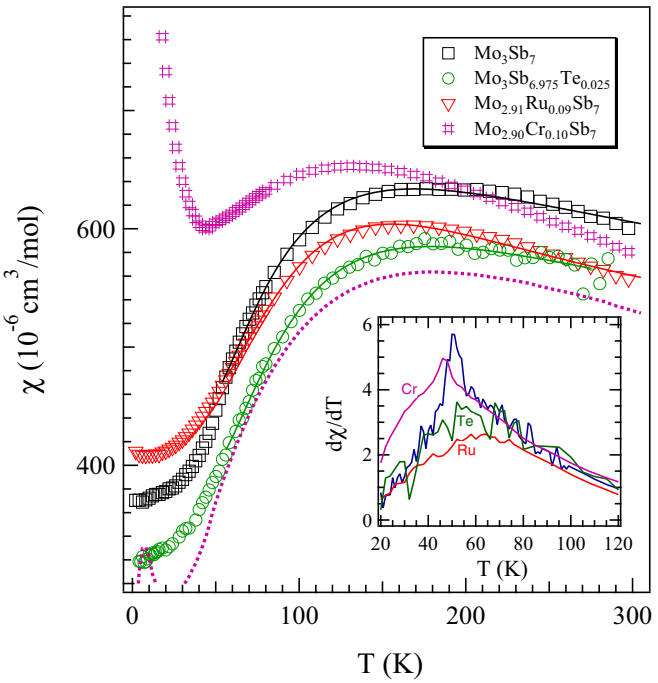

FIG. 2. (Color online) Temperature dependence of magnetic susceptibility measured with a magnetic field of 60 kOe. The dashed curve shows the magnetic susceptibility of $Mo_{2.90}Cr_{0.10}Sb_7$ after subtracting the low-temperature Curie-Weiss tail. The solid curves are fittings with the models described in text. The inset shows the temperature derivative of magnetic susceptibility, $d\chi(T)/dT$. $d\chi(T)/dT$ for $Mo_{2.90}Cr_{0.10}Sb_7$ was obtained from the dashed curve. Data for Mo_3Sb_7 are replotted from Ref. [18].

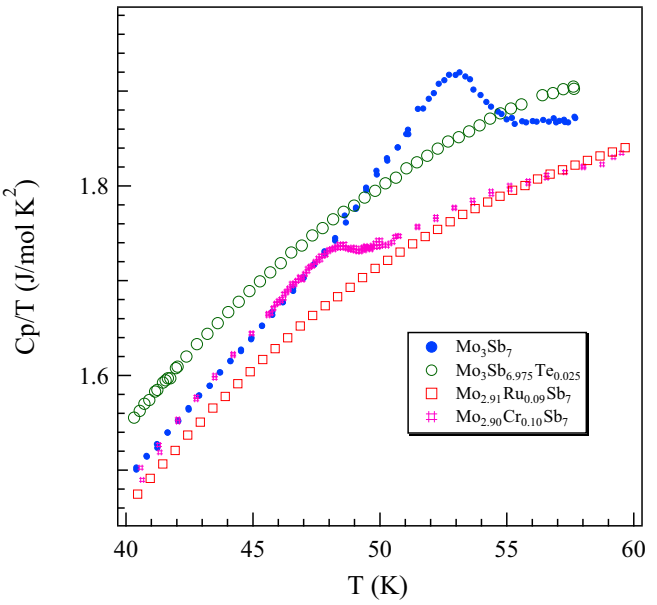

FIG. 3. (Color online) Temperature dependence of specific heat of doped Mo_3Sb_7 single crystals. Data for Mo_3Sb_7 are replotted from Ref. [18].

40 K in $\chi(T)$. This is as expected since Cr has a larger localized moment than Mo. The magnetic moment on Cr ions was estimated to be 1.1 μ_B/Cr by fitting the low-temperature CW tail. It is worth mentioning that the strong CW tail is inherent to the $Mo_{2.90}Cr_{0.10}Sb_7$ crystals and comes mainly from the isolated Cr spins. The broken Mo-Mo dimers by the Cr substituent may have a small contribution to the low-temperature CW tail, as evidenced by the low-temperature $\chi(T)$ of $Mo_{2.91}Ru_{0.09}Sb_7$.

Below 20 K, $\chi(T)$ curves for other compositions show little temperature dependence, which signals the good quality of our crystals. At high temperatures, a broad maximum was observed for all compositions. The broad maximum occurs at approximately $T_{max} = 175$ K for Mo_3Sb_7 and $Mo_3Sb_{6.975}Te_{0.025}$. For the other two compositions with substitution at the Mo site, the broad maximum shifts to lower temperatures.

$\chi(T)$ of Mo_3Sb_7 shows a rapid drop around $T_t = 53$ K, which leads to a distinct maximum around 53 K in the $d\chi/dT$ (inset of Fig. 2). For $Mo_{2.90}Cr_{0.10}Sb_7$, $d\chi/dT$ was obtained by first subtracting the low-temperature CW tail with $\chi_{CW} = C/(T-\theta)$, where C is the Curie constant and θ is the Weiss constant. A distinct maximum was observed around 48 K. In contrast, this feature becomes less distinguishable and only a broad maximum was observed around 50 K in $d\chi/dT$ of $Mo_3Sb_{6.975}Te_{0.025}$ and $Mo_{2.91}Ru_{0.09}Sb_7$.

Figure 3 shows the temperature dependence of specific heat plotted as $C_p(T)/T$ vs T around the structural transition. The slight difference in the magnitude of specific heat may come from the different Debye temperatures and/or experimental error. A weak λ anomaly near $T_t = 53$ K is well resolved for the parent compound. This anomaly becomes smaller in magnitude and shifts to ~48 K for $Mo_{2.90}Cr_{0.10}Sb_7$. In contrast, no anomaly was observed in the $C_p(T)/T$ curves in the normal state of $Mo_3Sb_{6.975}Te_{0.025}$ and $Mo_{2.91}Ru_{0.09}Sb_7$. The temperature dependence of $C_p(T)$ and $d\chi/dT$ suggests the structural transition disappears in $Mo_3Sb_{6.975}Te_{0.025}$ and $Mo_{2.91}Ru_{0.09}Sb_7$.

To confirm the doping effect on the structural transition of Mo_3Sb_7, the evolution with temperature of the cubic (800) peak was studied on oriented single crystals in the temperature interval $10 \leqslant T \leqslant 100$ K. As shown in Fig. 4, the (800) peak splits below 54 K signaling the lowering of the symmetry from cubic to tetragonal for Mo_3Sb_7. This peak splitting was observed at ~48 K for $Mo_{2.90}Cr_{0.10}Sb_7$. In sharp contrast, no peak splitting was observed for $Mo_3Sb_{6.975}Te_{0.025}$ and $Mo_{2.91}Ru_{0.09}Sb_7$. The x-ray diffraction experiments provide direct and unambiguous evidence for (1) the absence of the structural transition in $Mo_3Sb_{6.975}Te_{0.025}$ and $Mo_{2.91}Ru_{0.09}Sb_7$, and (2) the suppression of structural transition to 48 K in $Mo_{2.90}Cr_{0.10}Sb_7$. These results are consistent with other bulk properties. At 11 K, the a/c ratio was obtained to be 1.002 for both Mo_3Sb_7 and $Mo_{2.90}Cr_{0.10}Sb_7$.

The absence of a structural transition in $Mo_{2.91}Ru_{0.09}Sb_7$ and $Mo_3Sb_{6.975}Te_{0.025}$ is rather unusual. The shift of T_{max} in $\chi(T)$ curves to lower temperatures signals that the Mo-Mo antiferromagnetic interaction is disturbed by the random distribution of Ru or Cr at Mo site and possible breaking of Mo-Mo dimers. From this point of view, the substitution at Mo site should suppress the structural transition. This is supported by the case of $Mo_{2.90}Cr_{0.10}Sb_7$, where 3 at.% Cr doping suppresses the structural transition from 53 K in parent compound to 48 K. However, no sign of the structural transition was

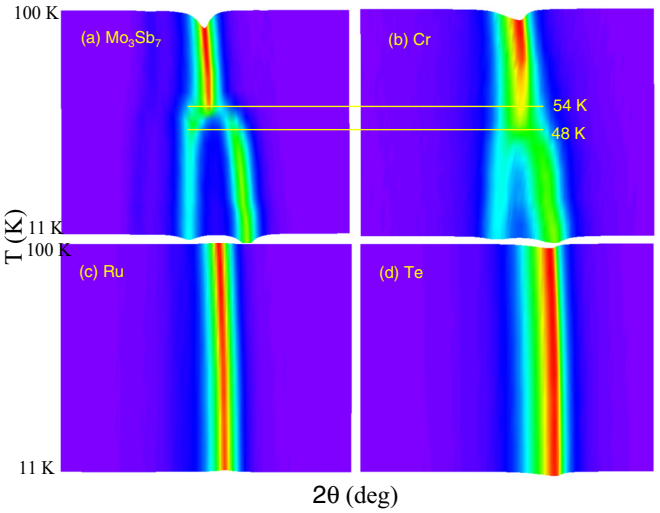

FIG. 4. (Color online) Temperature dependence of (800) reflections for (a) Mo_3Sb_7, (b) $Mo_{2.90}Cr_{0.10}Sb_7$, (c) $Mo_{2.91}Ru_{0.09}Sb_7$, and (d) $Mo_3Sb_{6.975}Te_{0.025}$. The data were collected on oriented single crystals.

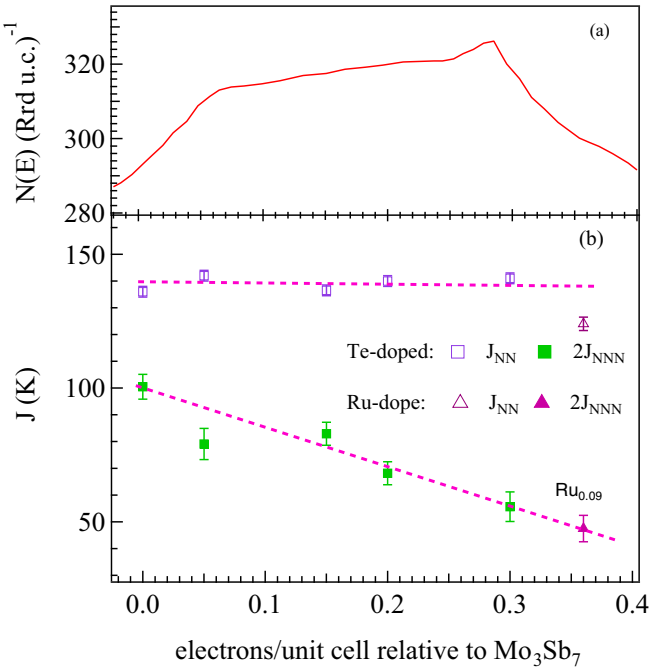

FIG. 5. (Color online) The evolution with extra electrons of (a) the electron DOS at the Fermi level, and (b) J_{NN} (open symbols) and J_{NNN} (solid symbols). The number of additional electrons is determined by integrating the density-of-states, which amounts to the assumption of rigid band behavior in the addition of dopants such as Ru or Te. Dashed lines in (b) are a guide to the eyes.

observed above T_c for $Mo_{2.91}Ru_{0.09}Sb_7$, where similar amount of Mo is replaced by Ru, from the temperature dependence of magnetization, specific heat, electrical resistivity (not shown), and x-ray diffraction. Therefore, disturbing the Mo sublattice by substitution at the Mo site does not drive the suppression of the structural transition in Mo_3Sb_7. The doping effect of Te on the structural transition further supports the above conclusion.

Substitution of Sb by Te does not disturb the Mo sublattice directly. However, as in $Mo_{2.91}Ru_{0.09}Sb_7$, no structural transition was observed by x-ray diffraction above 11 K and no anomaly associated with the structural transition was observed in the temperature dependence of magnetization, specific heat, and electrical resistivity in the normal state. Thus, Te substitution affects the structural transition in a way similar to that of Ru substitution although they reside at different crystallographic sites. Considering both dopants introduce additional electrons, we suggest that the structural transition is sensitive to electron concentration.

A band Jahn-Teller effect was proposed to induce the structural instability in cubic superconductors such as A15 compounds [11]. However, our band structure calculations for Te- and Ru-doped compositions suggest that light doping induces little change of the degeneracy and curvature of the valence bands, consistent with previous reports [16,17]. Thus a band Jahn-Teller effect is unlikely to drive the structural transition in Mo_3Sb_7. The density-of-states with doping is presented in Fig. 5, and was calculated from the converged WIEN2K band structure, as performed and presented in Ref. [19]. The electron DOS at the Fermi level increases slightly with Te or Ru substitution in the doping range studied in this work. No dramatic change of the electron DOS at the Fermi level is induced by the light doping.

To further understand how Ru or Te dopants affect the structural transition, the magnetic susceptibility data are analyzed in more detail. A previous study measuring $^{121/123}$Sb nuclear quadrupole resonance and muon spin relaxation of Mo_3Sb_7 suggested the importance of the interdimer magnetic interactions [6]. The Mo-Mo magnetic interactions between the nearest neighbors (J_{NN}) (i.e., the intradimer interaction) and next nearest neighbors (J_{NNN}) were estimated by fitting the $\chi(T)$ data above T_t with the mean-field modification of the Bleaney-Bowers equation [5,20–22]:

$$\chi(T) = \chi_0 + \frac{N_A \mu_B{}^2 g^2}{k_B T[3 + \exp(2J/k_B T) + J'/k_B T]}, \quad (1)$$

where χ_0 is a temperature independent term, N_A is the Avogadro number, μ_B is the Bohr magneton, k_B is the Boltzmann constant, $J = J_{NN}$ is the intradimer interaction, and J' is the interdimer interaction beyond the nearest Mo-Mo neighbors. The interdimer interaction includes the interaction J_{NNN} between next-nearest neighbors with a Mo-Mo distance of 4.642 Å and the interaction J_1 between the chains with a Mo-Mo distance of 5.220 Å [18]. Thus the interdimer interaction can be written as $J' = 8J_{NNN} + 4J_1$. With the assumption of J proportional to the Mo-Mo distance, J_1 can be estimated as $0.88J_{NNN}$ [5]. The obtained magnetic interactions are shown in Fig. 5 as a function of extra electrons. The following features are noteworthy: (1) the intradimer interaction J_{NN} is suppressed by partial substitution of Mo with Ru, but not by Sb with Te. This agrees with an intuitive picture that Te substitution disturbs only the Sb sublattice. J_{NN} shows little dependence on Te doping, indicating the absence of structural transition in doped compositions is not driven by J_{NN}; (2) substitution at either Mo or Sb site rapidly suppresses J_{NNN}; and (3) a larger suppression of J_{NNN} (~50%) is in contrast to a smaller suppression of J_{NN} (~10%) in $Mo_{2.91}Ru_{0.09}Sb_7$.

Considering that the structural transition disappears in both Te- and Ru-doped compositions, we suggest that the structural instability is very sensitive to J_{NNN}. The absence of the structural transition in 0.36% Te-doped composition signals that J_{NNN} in Mo_3Sb_7 is near a critical value and any electron doping that suppresses J_{NNN} would remove the structural instability.

For the $\chi(T)$ of $Mo_{2.90}Cr_{0.10}Sb_7$ we always observe the anomaly around 48 K in the $d\chi/dT$ curve when we fit the low-temperature CW term with different parameters. However, J_{NN} and J_{NNN} determined using Eq. (1) depend on the low-temperature CW term. Therefore, unfortunately, we cannot extract reliable J from fitting $\chi(T)$ of $Mo_{2.90}Cr_{0.10}Sb_7$.

The temperature dependence of magnetization, electrical resistivity, and specific heat shown in Fig. 1 clearly demonstrates that all dopants suppress T_c. The absence of superconductivity in $Mo_{2.90}Cr_{0.10}Sb_7$ above $T \geqslant 1.8$ K suggests that the superconductivity in Mo_3Sb_7 is sensitive to magnetic dopants [23]. Together with the fact that light Ru and Te doping suppresses superconductivity but increases the DOS at E_F, we can conclude that the superconductivity in Mo_3Sb_7 is sensitive to disorder and/or magnetic dopants as in cuprates. This makes it difficult to understand how the superconductivity reacts to the suppressed J_{NNN} by Te or Ru doping. The occurrence of superconductivity in the cubic phase of $Mo_3Sb_{6.975}Te_{0.025}$ and $Mo_{2.91}Ru_{0.09}Sb_7$ and the tetragonal phase of Mo_3Sb_7, and the absence of superconductivity in the tetragonal phase of $Mo_{2.90}Cr_{0.10}Sb_7$ observed in this study suggest that the tetragonal phase is not necessary for the superconductivity.

IV. SUMMARY

In summary, the effects of light doping of Mo_3Sb_7 with Ru, Cr, or Te have been studied in single crystals grown by a self-flux technique. All dopants suppress superconductivity. Superconductivity in Mo_3Sb_7 is sensitive to magnetic dopants and disorder but can exist in both cubic and tetragonal phases. The structural transition is extremely sensitive to additional electrons introduced by Te or Ru substitution. Analysis of the magnetic susceptibility data suggests that the interdimer magnetic interaction J_{NNN} is essential for the structural transition and is close to a critical value in Mo_3Sb_7. Our study highlights the importance of magnetism in the structural transition of Mo_3Sb_7. The sensitivity of the structural transition to electron doping and superconductivity to substitution suggests that hydrostatic pressure would be a cleaner tool to tune the ground state and to explore the correlation between structure, magnetism, and superconductivity in Mo_3Sb_7.

ACKNOWLEDGMENT

This research was supported by the U.S. Department of Energy, Office of Science, Basic Energy Sciences, Materials Sciences and Engineering Division.

[1] Z. Bukowski, D. Badurski, J. Stepien-Damm, and R. Troc, Solid State Commun. **123**, 283 (2002).
[2] H. Okabe, S. Yano, T. Muranaka, and J. Akimitsu, J. Phys.: Conf. Ser. **150**, 052196 (2009).
[3] T. Koyamaa, H. Yamashitaa, T. Koharaa, Y. Tabatab, and H. Nakamurab, Mater. Res. Bull. **44**, 1132 (2009).
[4] B. Wiendlocha and M. Sternik, Intermetallics **53**, 150 (2014).
[5] V. H. Tran, W. Miiller, and Z. Bukowski, Phys. Rev. Lett. **100**, 137004 (2008).
[6] T. Koyama, H. Yamashita, Y. Takahashi, T. Kohara, I. Watanabe, Y. Tabata, and H. Nakamura, Phys. Rev. Lett. **101**, 126404 (2008).
[7] V. H. Tran, A. D. Hillier, D. T. Adroja, Z. Bukowski, and W. Miiller, J. Phys.: Condens. Matter **21**, 485701 (2009).
[8] C. Candolfi, B. Lenoir, A. Dauscher, C. Bellouard, J. Hejtmanek, E. Santava, and J. Tobola, Phys. Rev. Lett. **99**, 037006 (2007).
[9] B. Wiendlocha, J. Tobola, M. Sternik, S. Kaprzyk, K. Parlinski, and A. M. Oles, Phys. Rev. B **78**, 060507(R) (2008).
[10] V. H. Tran, R. T. Khan, P. Wisniewski, and E. Bauer, J. Phys.: Conf. Ser. **273**, 012088 (2011).
[11] L. R. Testardi, Rev. Mod. Phys. **47**, 637 (1975).
[12] D. C. Johnston, Adv. Phys. **59**, 803 (2010).
[13] A. S. Sefat, Rep. Prog. Phys. **74**, 124502 (2011).
[14] C. Candolfi, B. Lenoir, C. Chubilleau, A. Dauscher, and E. Guilmeau, J. Phys.: Condens. Matter **22**, 025801 (2010).
[15] C. Candolfi, J. Leszczynski, P. Masschelein, C. Chubilleau, B. Lenoir, A. Dauscher, E. Guilmeau, J. Hejtmanek, S. J. Clarke, and R. I. Smith, IEEE/TMS J. Electron. Mater. **39**, 2132 (2010).
[16] C. Candolfi, B. Lenoir, A. Dauscher, J. Hejtmanek, and J. Tobola, Phys. Rev. B **79**, 235108 (2009).
[17] C. Candolfi, B. Lenoir, A. Dauscher, J. Hejtmanek, and J. Tobola, Phys. Rev. B **80**, 155127 (2009).
[18] J.-Q. Yan, M. A. McGuire, A. F. May, H. B. Cao, A. D. Christianson, D. G. Mandrus, and B. C. Sales, Phys. Rev. B **87**, 104515 (2013).
[19] D. Parker, M. H. Du, and D. J. Singh, Phys. Rev. B **83**, 245111 (2011).
[20] B. Bleaney and K. D. Bowers, Proc. R. Soc. London Ser. A **214**, 451 (1952).
[21] T. Nakajima, H. Mitamura, and Y. Ueda, J. Phys. Soc. Jpn. **75**, 054706 (2006).
[22] Y. Chen, T. Liu, C. He, and C. Duan, J. Mater. Chem. **22**, 19872 (2012).
[23] M. B. Maple, Appl. Phys. **9**, 179 (1976).